

# Mathematical analysis of toluene biodegradation by rhodococcus erythropolis in bioreactor using new approach to homotopy perturbation method

<sup>1</sup>R. Karthikeyan, <sup>1</sup>A.P.Dhanabalan, <sup>2</sup>M. Rasi, <sup>3</sup>L.Rajendran

<sup>1</sup>PG and Research Department of Mathematics, Alagappa Govt Arts College, Karaikudi-630003, Tamilnadu.

<sup>2</sup>Department of Mathematics, Lady Doak College, Madurai-625007, India

<sup>3</sup>Department of Mathematics ' Academy of Maritime Education and Training (AMET),

Deemed to be University, Kanathur- 603112, India.

## Abstract

The mathematical model for toluene removal and CO<sub>2</sub> production by rhodococcus erythropolis has been discussed. This paper presents an analytical method (Homotopy perturbation method) to solve the nonlinear differential equations that describe the biomass formation, toluene mineralization, and CO<sub>2</sub> production in liquid and gas phase with respect to time. Approximate analytical expressions for the concentration of biomass formation, toluene mineralization, and CO<sub>2</sub> production in liquid and gas have been derived for various values of the relevant parameters. Our analytical results are compared with the experimental data. In addition, the sensitivity of the kinetic parameters was also analyzed.

**Keywords:** Toluene; CO<sub>2</sub> production; Rhodococcus erythropolis; Modeling; Homotopy perturbation method;

## Introduction

Pollution in the atmosphere has become one of the major cause of premature death in many countries [1]. It is due to the volatile organic compounds (VOCs), which are introduced into the atmosphere through anthropogenic or biogenic activities [2]. Nowadays several steps are taken to reduce the emission of volatile organic compounds (VOC) like toluene, nitric oxide, ethanol etc., because of its harmfulness towards to human. Among these VOCs, toluene occur in the commonly used consumer products such as paints, glues and nail polish removers.

Toluene is a clear, colorless liquid solvent with a distinctive smell. It occurs naturally in crude oil and in the tolu tree. It can be released into the air, water, and soil at places where it is produced or used and particularly in heavy vehicular traffic. Toluene can enter into the body by breathing outdoor or indoor air containing this substance. It can affect your nervous system (brain and nerves) such as headaches, dizziness, or unconsciousness. However, effects such as incoordination, cognitive impairment, and vision and hearing loss may become permanent. High levels of toluene exposure during pregnancy, such as those associated with solvent abuse, may lead to retardation of mental abilities and growth in children. Other health effects of potential concern may include immune, kidney, liver, and reproductive effects. To control the release of VOC's like nitrous oxide, nitric oxide, toluene etc. from industries, biofilters are being used instead of the chemical complex absorption method [3].

Biofilters have dual role: one is reducing the turbidity and pathogen particles like the conventional filters, and the other is removing the biodegradable organic matter (BOM) and other bioavailable materials through the microbial metabolism of the biofilm attached to the media.[4]. Many researchers have conducted experimental studies for removal of VOC's (toluene) using biofiltration [5,6]. Biotrickling filtration is a potential and cost effective alternative for the treatment of VOC emission in air, so it is necessary to deepen into the key aspects of design and operation for the optimization of this technology [7].

Mathematical modeling is widely used for optimize and investigate in order to reduce the number of physical experiments required during the removal of volatile organic compounds. Recently, Malhautier et al. [8] developed a mathematical model for the characterization of kinetic parameters in the biodegradation of toluene by *Rhodococcus erythropolis* in a bioreactor. To the best of our knowledge, there are no rigorous approximate analytical solutions presented for the concentrations of substrate, biomass and CO<sub>2</sub> in liquid and gas phase. The main aim of this article is to find the approximate analytical expressions for the concentrations of substrate, biomass and CO<sub>2</sub> in liquid and gas phase.

### Mathematical model

The system of nonlinear ordinary differential equations under consideration is as follows [8] :

$$\frac{dCO_{2L}(t)}{dt} = \alpha \frac{dX(t)}{dt} + \beta X(t) \tag{1}$$

$$\frac{dCO_{2G}(t)}{dt} = \frac{dCO_{2L}(t)}{dt} H_{CO_2} \tag{2}$$

$$\frac{dS(t)}{dt} = -\frac{\mu(S)}{Y_{X/S}} X(t) \tag{3}$$

$$\frac{dX(t)}{dt} = \mu(S)X(t) \tag{4}$$

Where

$$\mu(S) = \frac{\mu_{max}S}{K_S + S + \frac{S^2}{K_I}} \tag{5}$$

(5)

is the specific growth rate. The initial conditions for Eqs. (1) – (4) are represented as follows:

$$\text{At } t = 0, CO_{2L}(t) = CO_{2L_0}, \quad CO_{2G}(t) = CO_{2G_0}, \quad S(t) = S_0, \quad X(t) = X_0$$

(6) Using Eq. (3) and (4), the following linear differential equation can be obtained.

$$\frac{d}{dt} [Y_{X/S}S(t) + X(t)] = 0 \tag{7}$$

The exact solution of equation (7) is

$$S(t) = S_0 + \frac{X_0}{Y_{X/S}} - \frac{X(t)}{Y_{X/S}} \tag{8}$$

Eqn. (8) provides the relationship between the substrate and the biomass concentration. The plot of  $S(t)$  versus  $X(t)$  gives the intercept  $S_0 + \frac{X_0}{Y_{X/S}}$  and slope  $-\frac{1}{Y_{X/S}}$ . The yield coefficient of substrate utilization  $Y_{XS}$  can be calculated from these parameters. The other parameters  $\mu_{max}$  and  $K_S$  can be estimated from the linear plot of  $\frac{1}{\mu(S)}$  versus  $\frac{1}{S}$  using the equation  $\mu(S) = \mu_{max}S / (K_S + S + S^2 / K_I)$  [9].

#### Approximate analytical solution for Eqs. (1) – (4) using a new approach to the Homotopy perturbation method.

In recent years, solving system of nonlinear ordinary differential equations have gained importance due to the need of the analytical solutions various fields of science and engineering. Most researchers have contributed to the study of solutions

of nonlinear ordinary differential equations by applying various analytical techniques like variational iteration method [10], Homotopy analysis method [11], Homotopy perturbation method [12], Laplace Adomian decomposition method [13], a new approach to Homotopy perturbation method [14] etc. Among these a new approach to the Homotopy perturbation method was applied to solve the nonlinear ordinary differential equations Eqs. (1) – (4). The advantage of this method is that it provided a simple approximate solution in the zeroth iteration itself [15]. Using this method the concentration of biomass  $X(t)$  is obtained as follows (Appendix A):

$$X(t) = \frac{X_0 X_{SS}}{X_0 + S_0 Y_{X/S} e^{-At}}$$

(9)

Substituting Eq. (9) in the Eq. (8), the concentration of substrate  $S(t)$  can be obtained as follows:

$$S(t) = S_0 + \frac{X_0}{Y_{X/S}} - \frac{X_0 X_{SS}}{Y_{X/S}(X_0 + S_0 Y_{X/S} e^{-At})}$$

(10)

The concentration of CO<sub>2</sub> in liquid  $CO_{2L}(t)$  and gas phase  $CO_{2G}(t)$  can be obtained using Eq. (1), (2) and (9).

$$CO_{2L}(t) = CO_{2L0} + \left[ \alpha + \frac{\beta}{\mu_{max}} \left( \frac{K_S}{S_0} + \frac{S_0}{K_I} + 1 \right) \right] \left[ \frac{(X_0 + S_0 Y_{X/S}) X_0}{X_0 + S_0 Y_{X/S} e^{-At}} - X_0 \right]$$

(11)

$$CO_{2G}(t) = CO_{2G0} + H(CO_{2L}(t) - CO_{2L0})$$

(12)

where the parameter

$$A = X_{SS} \mu_{max} / Y_{X/S} (K_S + S_0 + S_0^2 / K_I)$$

(13)

and

$$X_{SS} = X_0 + S_0 Y_{X/S}$$

(14)

$$S_{SS} = 0$$

(15)

$$CO_{2LSS} = CO_{2L0} + \left[ \alpha + \frac{\beta}{\mu_{max}} \left( \frac{K_S}{S_0} + \frac{S_0}{K_I} + 1 \right) \right] S_0 Y_{X/S}$$

(16)

$$CO_{2GSS} = CO_{2G0} + H \left[ \alpha + \frac{\beta}{\mu_{max}} \left( \frac{K_S}{S_0} + \frac{S_0}{K_I} + 1 \right) \right] S_0 Y_{X/S}$$

(17)

are the steady state solution of biomass, substrate and CO<sub>2</sub> in liquid and gas phase respectively.

## Discussion

Eqs. (9) – (12) represents the simple analytical expression for the concentration of biomass, liquid toluene, CO<sub>2</sub> concentration in liquid phase and CO<sub>2</sub> concentration in gas phase respectively in terms of the kinetic parameters  $\mu_{max}$ ,  $K_S$ ,  $K_I$ ,  $Y_{X/S}$ ,  $\alpha$  and  $\beta$ . Fig. 1 shows the comparison of analytical results with numerical simulation for the concentration of liquid toluene and Gaseous CO<sub>2</sub> for experimental values of kinetic parameters.

\*\*\***(Figure 1)**\*\*\*

To analyze and predict the influence of kinetic parameters for decreasing the emission of toluene, a sensitivity analysis was calculated for experimental values of the parameters in Fig. 2(a) and 2(b). From the figure, it is evident that the parameters like to  $\mu_{max}$ ,  $K_S$ ,  $K_I$  and  $Y_{X/S}$  has the same level of influence over the concentration of biomass, liquid CO<sub>2</sub> and gaseous CO<sub>2</sub>. But for liquid toluene, they have different percentage level. The percentage of change in biomass, liquid CO<sub>2</sub> and gaseous CO<sub>2</sub> with respect to  $\mu_{max}$ ,  $K_S$ ,  $K_I$  and  $Y_{X/S}$  is 87%, -3%, 0.02% and 15.98% respectively. The negative sign indicates that the concentration increases when the toluene half saturation constant decreases. The percentage of change in concentration of liquid toluene (substrate) with respect to  $\mu_{max}$ ,  $K_S$  and  $K_I$  is 103%, -3.03% and 0.03% respectively. The main variable of interest in this study is  $\mu_{max}$ , because of its high level of impact on the concentration of biomass, substrate, liquid CO<sub>2</sub> and gaseous CO<sub>2</sub>.

\*\*\***(Figure 2)**\*\*\*

Fig. 3(a) – (d) shows the concentration of biomass  $X(t)$  versus time  $t$  for various values of maximum specific biomass growth rate  $\mu_{max}$ , toluene half saturation constant  $K_S$ , toluene inhibition constant  $K_I$  and biomass to toluene yield coefficient  $Y_{X/S}$  respectively. From Fig. 3(a), it is evident that when the maximum specific growth rate increases, the concentration of biomass increases and reaches its steady state value for short interval of time. From Fig. 3(b)-3(d), it is inferred that the parameter  $K_S$  is inversely proportional to the concentration of biomass where as  $K_I$  and  $Y_{X/S}$  is directly proportional to biomass. And variation in  $K_S$  doesn't show much deviation in biomass concentration compared to other parameters  $\mu_{max}$ ,  $K_I$  and  $Y_{X/S}$ . Fig. 3(d) shows that different value of biomass is obtained for different of substrate utilization yield  $Y_{X/S}$ . This is because the steady state value of biomass  $X_{SS}$  depends upon the value of  $Y_{X/S}$ , i.e.  $X_{SS} = X_0 + S_0 Y_{X/S}$ .

\*\*\***(Figure 3)**\*\*\*

The influence of kinetic parameters over substrate concentration with respect to time  $t$  for are illustrated in Fig. 4(a) – (c) respectively. From Fig. 4(a) and 4(c), it is evident that the degradation of the substrate increases for increase in biomass growth rate  $\mu_{max}$ , toluene inhibition constant  $K_I$  and decrease in toluene half saturation constant  $K_S$ .

\*\*\***(Figure 4)**\*\*\*

The impact of kinetic parameters on CO<sub>2</sub> production in liquid phase and gas phase was illustrated in Fig. 5 and 6. From these figures, it is true that the kinetic parameters shows same level of influence on CO<sub>2</sub> in both liquid and gaseous phase.

\*\*\***(Figure 5 and 6)**\*\*\*

### Conclusion

A nonlinear mathematical model comprising a set of ordinary differential equation describing toluene degradation by rhodococcus erythropolis has been solved analytical in a rigorous mathematical approach using new approach to the Homotopy perturbation method. Approximate analytical expressions for biomass, liquid toluene, liquid CO<sub>2</sub> and gaseous CO<sub>2</sub> production were obtained. The obtained analytical results were compared with numerical simulation and it shows satisfactory agreement. Also the steady state solution of each concentration and the analytical relation between biomass and substrate are reported. The sensitivity analysis of the parameters is also presented in order to provide necessary information for parameter analyzation, control, model simplification and experimental design.

#### Appendix A: Approximate analytical solutions for Eq. (1) using HPM.

Using the relation Eq. (6), Eq. (1) can be written as

$$\frac{dX(t)}{dt} = \frac{\mu_{max}X(t)[S_0Y_{xS}+X_0-X(t)]}{K_S+S(t)+S(t)^2/K_I} \tag{A.1}$$

In order to solve Eq. (1), construct the homotopy as follows:

$$(1 - p) \left\{ \frac{dX(t)}{dt} - B[S_0Y_{xS} + X_0 - X(t)]X(t) \right\} + p \left[ \frac{dX}{dt} (K_S + S(t) + \frac{S(t)^2}{K_I}) - \mu_{max}S(t)X(t) \right] = 0 \tag{A.2}$$

Where

$$B = \frac{\mu_{max}}{K_S+S(0)+S(0)^2/K_I}$$

(A.3)

The approximate solution of (A.2) is as follows:

$$X = X_{zeroth} + pX_{first} + p^2X_{second} + \dots \tag{A.4}$$

Substituting (A.4) in Eq. (A.2) and equating the like powers of  $p$

$$p^0 : \frac{dX_{zeroth}(t)}{dt} - B[S_0 Y_{xS} + X_0 - X_{zeroth}(t)]X_{zeroth}(t) = 0$$

(A.5)

The initial condition for the above equation is

$$\text{At } t = 0, X_{zeroth}(0) = X_0$$

(A.6)

Solving Eq. (A.5),  $X_{zeroth}(t)$  can be obtained as follows

$$X_{zeroth}(t) = \frac{X_0 X_{SS}}{X_0 + S_0 Y_{xS} e^{-At}}$$

(A.7)

Where  $A = X_{SS} \mu_{max} / Y_{X/S} (K_S + S_0 + S_0^2 / K_I)$  and  $X_{SS} = X_0 + S_0 Y_{xS}$

(A.8)

Substituting (A.7) in Eq. (A.2),  $X(t) \approx X_{zeroth}(t)$  which is the Eq. (7) in the text.

**Symbols used**

| Symbols     | Unit                   | Meaning  |
|-------------|------------------------|--|
| $CO_{2G}$   | (g m <sup>-3</sup> )   | CO <sub>2</sub> concentration in gas phase             |
| $CO_{2G_0}$ | (g m <sup>-3</sup> )   | initial CO <sub>2</sub> concentration in liquid phase  |
| $CO_{2L}$   | (g m <sup>-3</sup> )   | CO <sub>2</sub> concentration in liquid phase          |
| $CO_{2L_0}$ | (g m <sup>-3</sup> )   | initial CO <sub>2</sub> concentration in liquid phase  |
| $H_{CO_2}$  | (g m <sup>-3</sup> )   | dimensionless Henry's law constant for CO <sub>2</sub> |
| $K_I$       | (g m <sup>-3</sup> )   | toluene inhibition constant                            |
| $K_S$       | (g m <sup>-3</sup> )   | toluene half saturation constant                       |
| $S$         | (g m <sup>-3</sup> )   | Concentration of substrate                             |
| $S_0$       | (g m <sup>-3</sup> )   | Initial concentration of substrate                     |
| $t$         | (h)                    | Time   |
| $X$         | (g m <sup>-3</sup> )   | Concentration of biomass (Bacteria)                    |
| $X_0$       | (g m <sup>-3</sup> )   | Initial concentration of biomass (Bacteria)            |
| $Y_{X/S}$   | (gX gS <sup>-1</sup> ) | biomass to toluene yield                               |

**Greek symbols**

|             |                                      |                                       |
|-------------|--------------------------------------|---------------------------------------|
| $\mu$       | (h <sup>-1</sup> )                   | specific biomass growth rate          |
| $\mu_{max}$ | (h <sup>-1</sup> )                   | maximum specific biomass growth rate  |
| $\alpha$    | (gCO <sub>2</sub> gX <sup>-1</sup> ) | constant of the Luedeking-Piret model |
| $\beta$     | (gCO <sub>2</sub> gX <sup>-1</sup> ) | constant of the Luedeking-Piret model |

**Subscripts**

|       |                             |
|-------|-----------------------------|
| 0     | Initial concentration       |
| $max$ | Maximum                     |
| $S$   | Substrate                   |
| $SS$  | Steady state                |
| $X/S$ | Substrate utilization yield |

## References

- [1] A.Vergara-Fernández, S. Revah, P. Moreno-Casas, F. Scott, *Biofiltration of volatile organic compounds using fungi and its conceptual and mathematical modelling*, *Biotechnology Advances*, Volume 36, Issue 4, July–August 2018, Pages 1079-1093.
- [2] R. Montero-Montoya, *Volatile Organic Compounds in Air: Sources, Distribution, Exposure and Associated Illnesses in Children*. *Annals of Global Health*. 2018; 84(2), pp. 225–238.
- [3] L.Vafajoo, A. Naserranjbar, F. Khorasheh, Farhad, 2012. In: *A Mathematical Model for Removal of VOC's from Polluted Air Utilizing a Biofilter*, *Chemical Engineering Transactions, MATLAB 6.1*, vol. 29. The MathWorks Inc., Natick, MA, p. 2000.
- [4] Yu Xin, Ye Lin, Wei Gu, *Modeling the formation of soluble microbial products(SMP) in drinking water biofiltration*, *Water Science and Engineering*, Sep. 2008, Vol. 1, No. 3, 93-101.
- [5] M. Srikumar, S. Papita Das , B. Divya, R. Ravi, *Microbial biofilter for toluene removal: Performance evaluation,transient operation and theoretical prediction of elimination capacity*, *Sustainable Environment Research*, Volume 28, Issue 3, May 2018, Pages 121-127.
- [6] M. Rasi Muthuramalingam, R. Sunil Kumar, L. Rajendran, *Analytical expressions for the concentrationof nitric oxide removal in the gas and biofilm phasein a biotrickling filter*, *Journal of the Association of Arab Universities for Basic and Applied Sciences*, Volume 18, October 2015, Pages 19-28.
- [7] P. San-Valero, C. Gabaldón, J. Peña-roja, M.C. Pérez, *Study of mass oxygen transfer in a biotrickling filter for air pollution control*, *Procedia Engineering* 42 ( 2012 ) 1726 – 1730.
- [8] L. Malhautier, G. Quijano, M. Avezac, J. Rocher, J.L. Fanlo, *Kinetic characterization of toluene biodegradation by Rhodococcus erythropolis: Towards a rationale for microflora enhancement in bioreactors devoted to air treatment*, *Chemical Engineering Journal* 247 (2014) 199–204.



[9] R. Sathya, M. Rasi, L. Rajendran, *Non-linear analysis of Haldane kinetic model in phenol*

*degradation in batch operations, Kinetics and Catalysis, 2015, 56 (2), 141-146.*

[10] A.M. Wazwaz, *The variational iteration method for solving linear and nonlinear ODEs and scientific models with variable coefficients, Central European Journal of Engineering. 2014, 4, 64-71.*

[11] M. Rasi, K. Indira, L. Rajendran, *Approximate Analytical Expressions for the Steady-State Concentration of Substrate and Cosubstrate over Amperometric Biosensors for Different Enzyme Kinetics International Journal of Chemical of Kinetics, 2013, 45, 322–336.*

[12] A. Meena, L. Rajendran, *Analysis of a pH-Based Potentiometric Biosensor Using the Homotopy Perturbation Method Chemical Engineering and Technology, 2010, 33, 1999-2007.*

[13] M.Y. Ongun, *The Laplace adomian decomposition method for solving a model for HIV infection of CD4<sup>+</sup>T cells, Mathematical and Computer Modelling, 2011, 53, 597-603.*

[14] N. Mehala, L. Rajendran, *Analysis of Mathematical Modelling on Potentiometric Biosensors, ISRN Biochemistry. 2014, Article ID 58275, 11 pages.*

[15] L. Rajendran, S. Anitha, *Reply to “Comments on analytical solution of amperometric enzymatic reactions based on Homotopy perturbation method,” by Ji-Huan He, Lu-Feng Mo [Electrochim. Acta (2013)] Electrochim. Acta. 2013, 102, 474-476.*

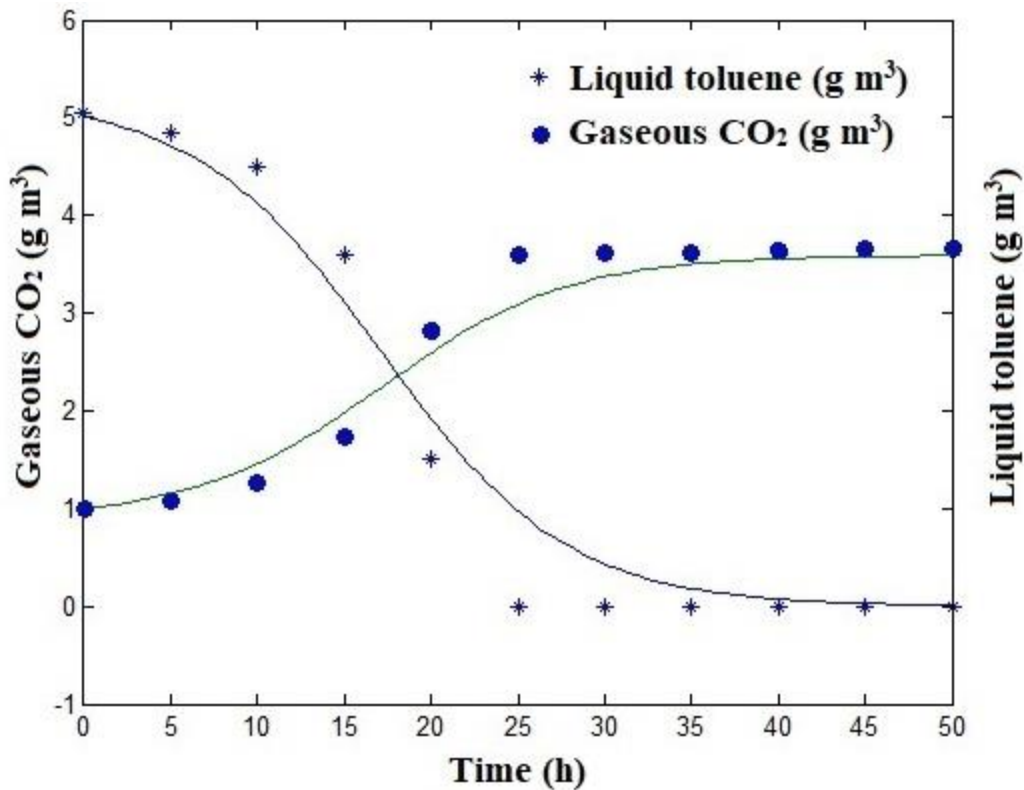


**Fig. 1** Comparison of numerical simulation (symbols) and analytical expression (solid line) [Eq. (10) and (12)] for the concentration of liquid toluene  $S(t)$  and carbon dioxide in gas phase  $CO_{2G}(t)$  respectively.

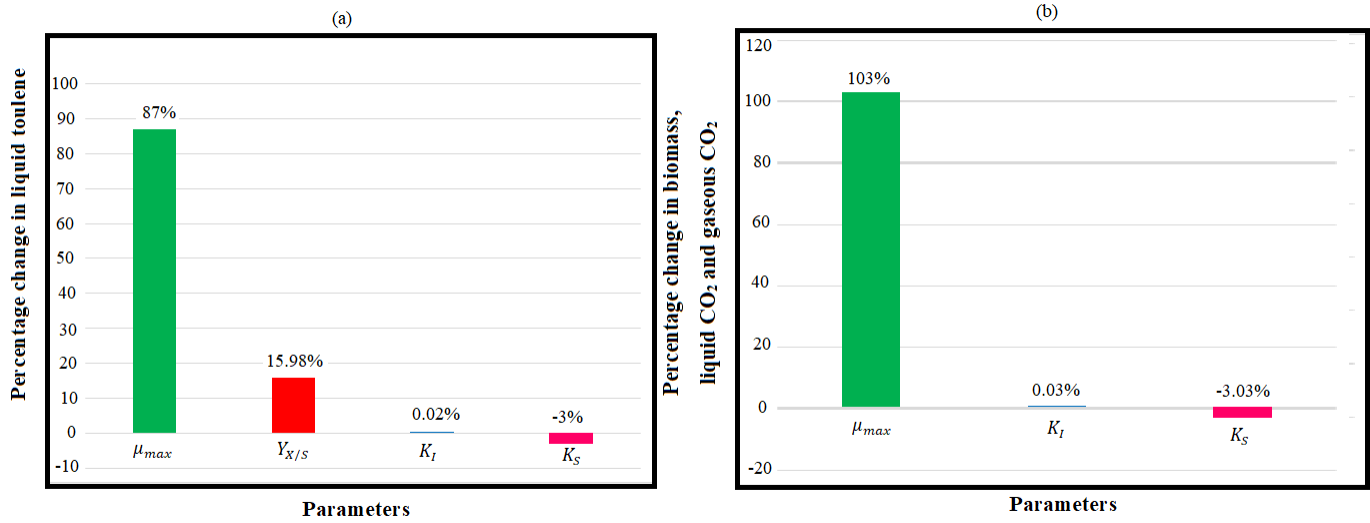


**Fig. 2** Percentage change in (a) liquid toluene (b) biomass, liquid CO<sub>2</sub> and gaseous CO<sub>2</sub> versus kinetic parameters.

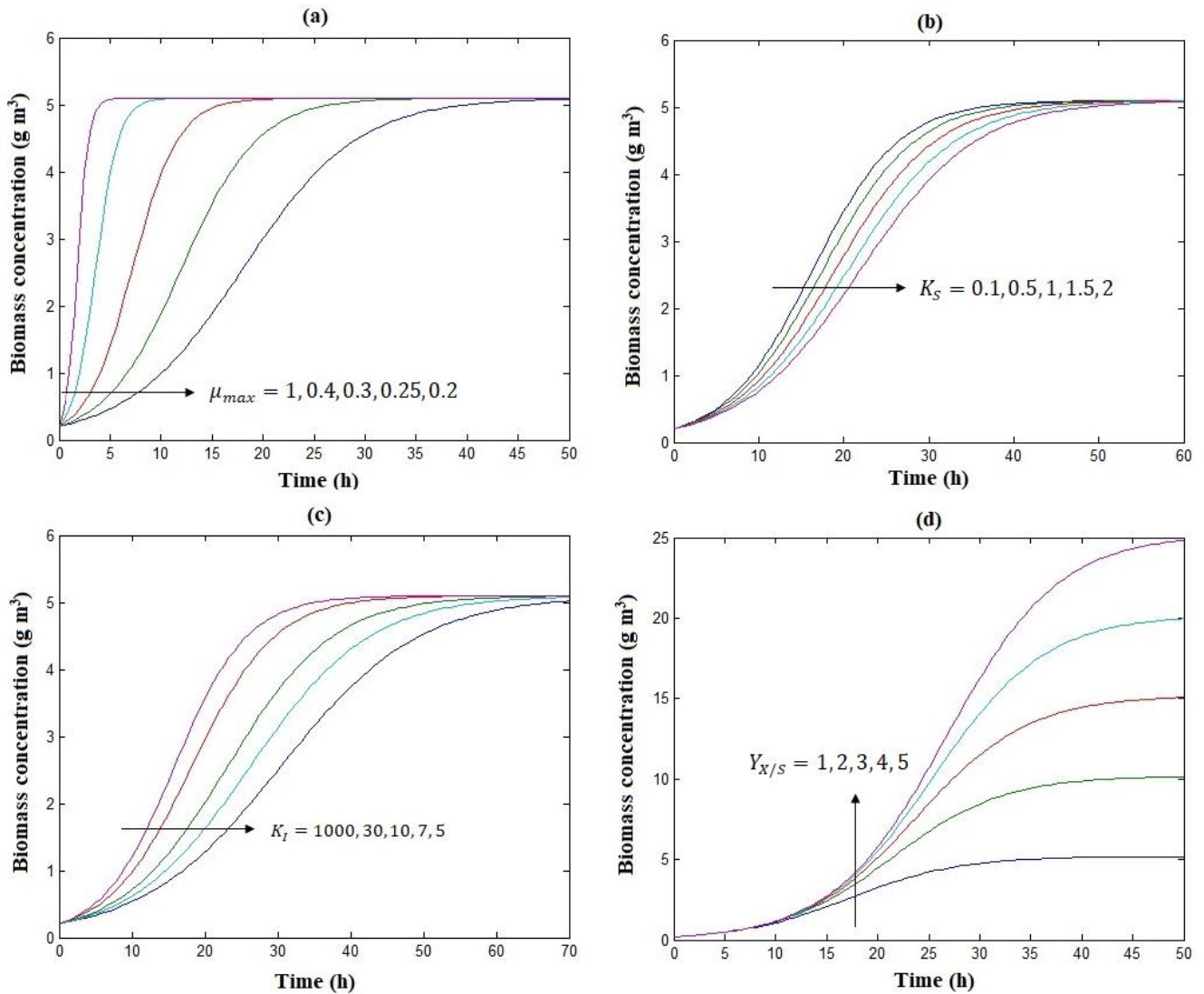


**Fig. 3** Concentration profile of biomass  $X(t)$  (Eq. (9)) versus time  $t$  for some experimental values of the parameters and for various values of (a) maximum specific growth rate  $\mu_{max}$  (b) toluene half saturation constant  $K_S$  (c) toluene inhibition constant  $K_I$  and (d) biomass to toluene yield  $Y_{X/S}$  respectively.

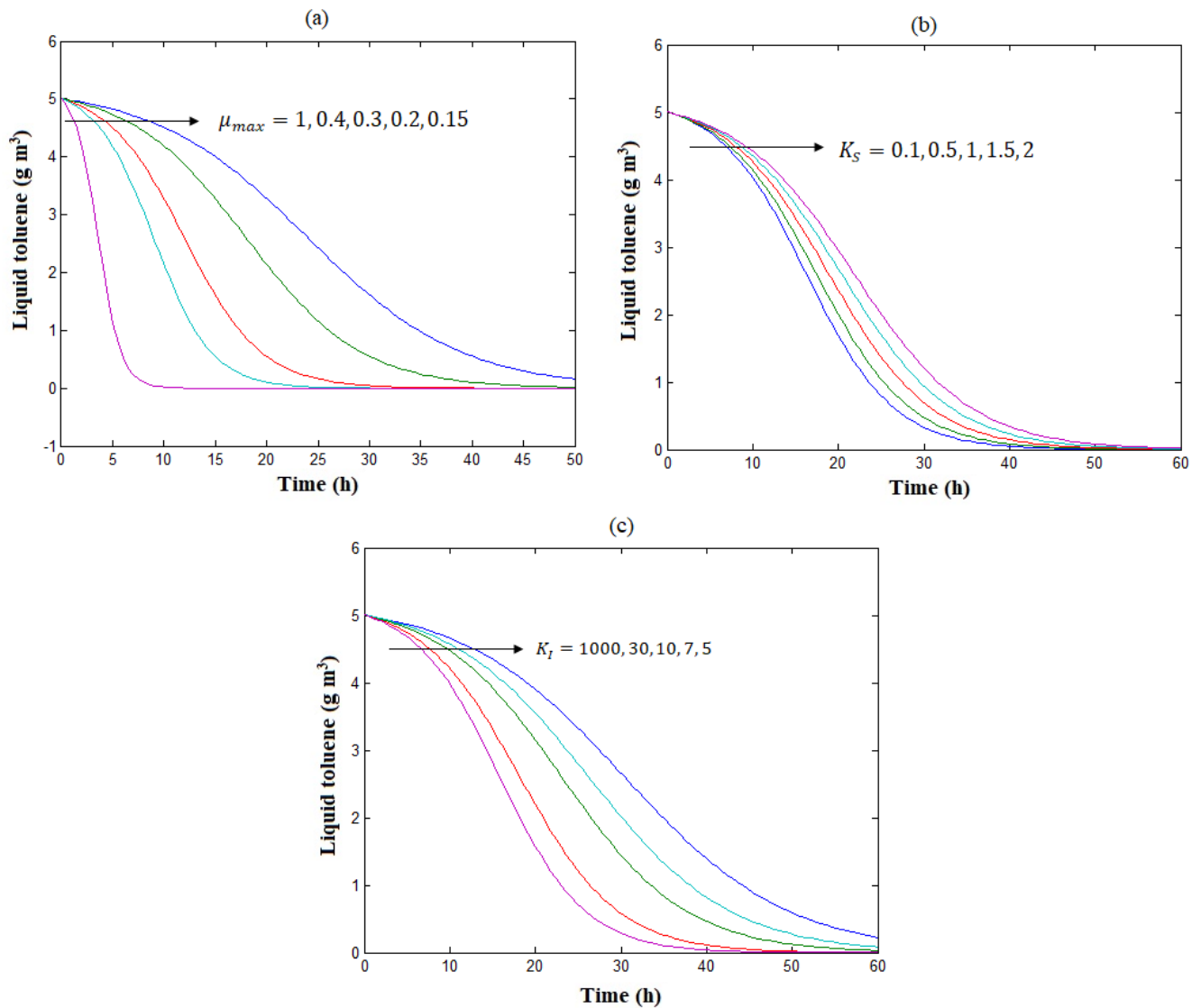


**Fig. 4** Concentration profile of substrate (liquid toluene)  $S(t)$  [Eq. (10)] versus time  $t$  for some experimental values of the parameters and for various values of (a) maximum specific growth rate  $\mu_{max}$  (b) toluene half saturation constant  $K_S$  and (c) toluene inhibition constant  $K_I$  respectively.

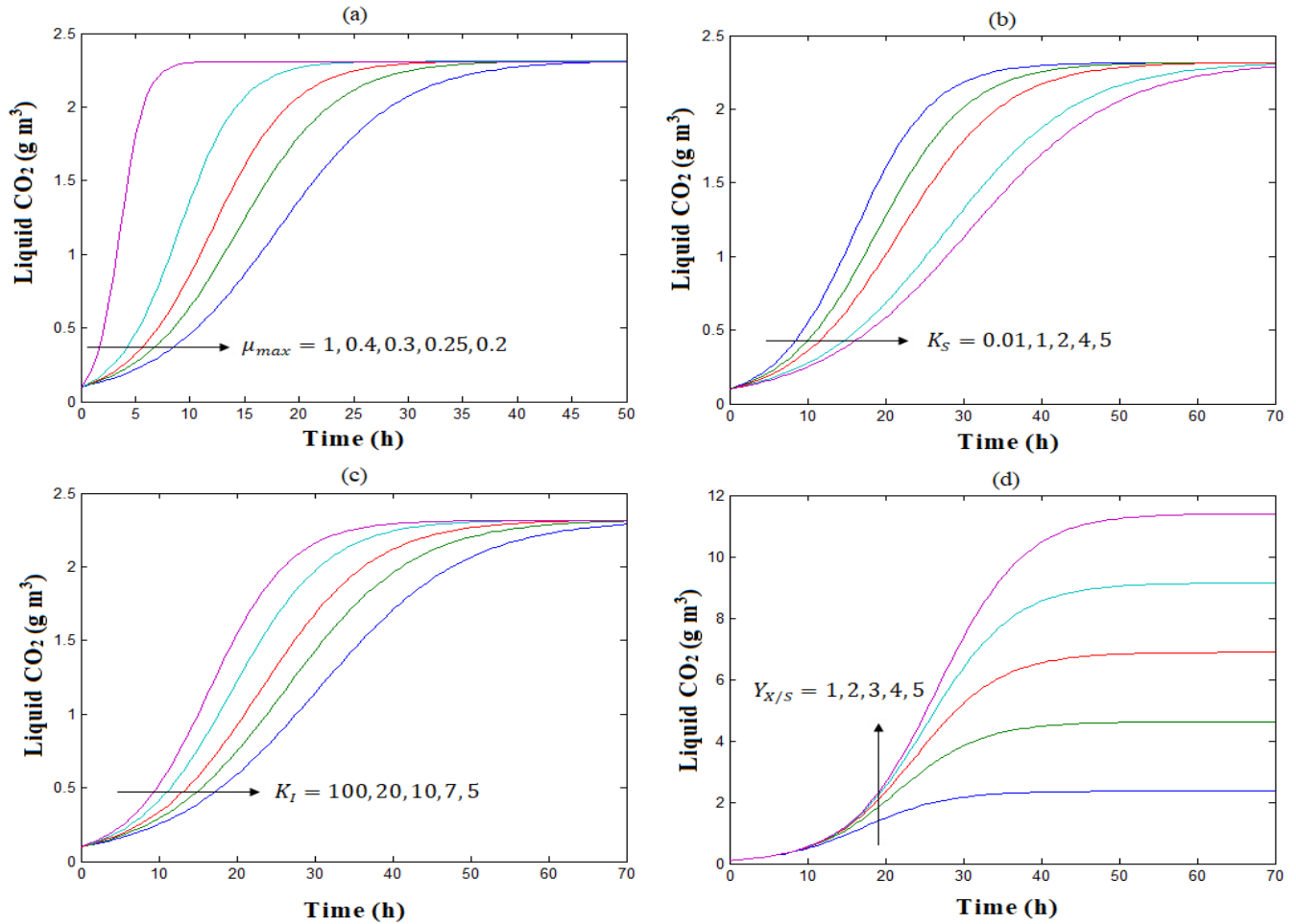


**Fig. 5** Concentration profile of liquid carbondioxide  $CO_{2L}(t)$  [Eq. (11)] versus time  $t$  for some experimental values of the parameters and for various values of (a) maximum specific growth rate  $\mu_{max}$  (b) toluene half saturation constant  $K_S$  (c) toluene inhibition constant  $K_I$  and (d) biomass to toluene yield  $Y_{X/S}$  respectively.

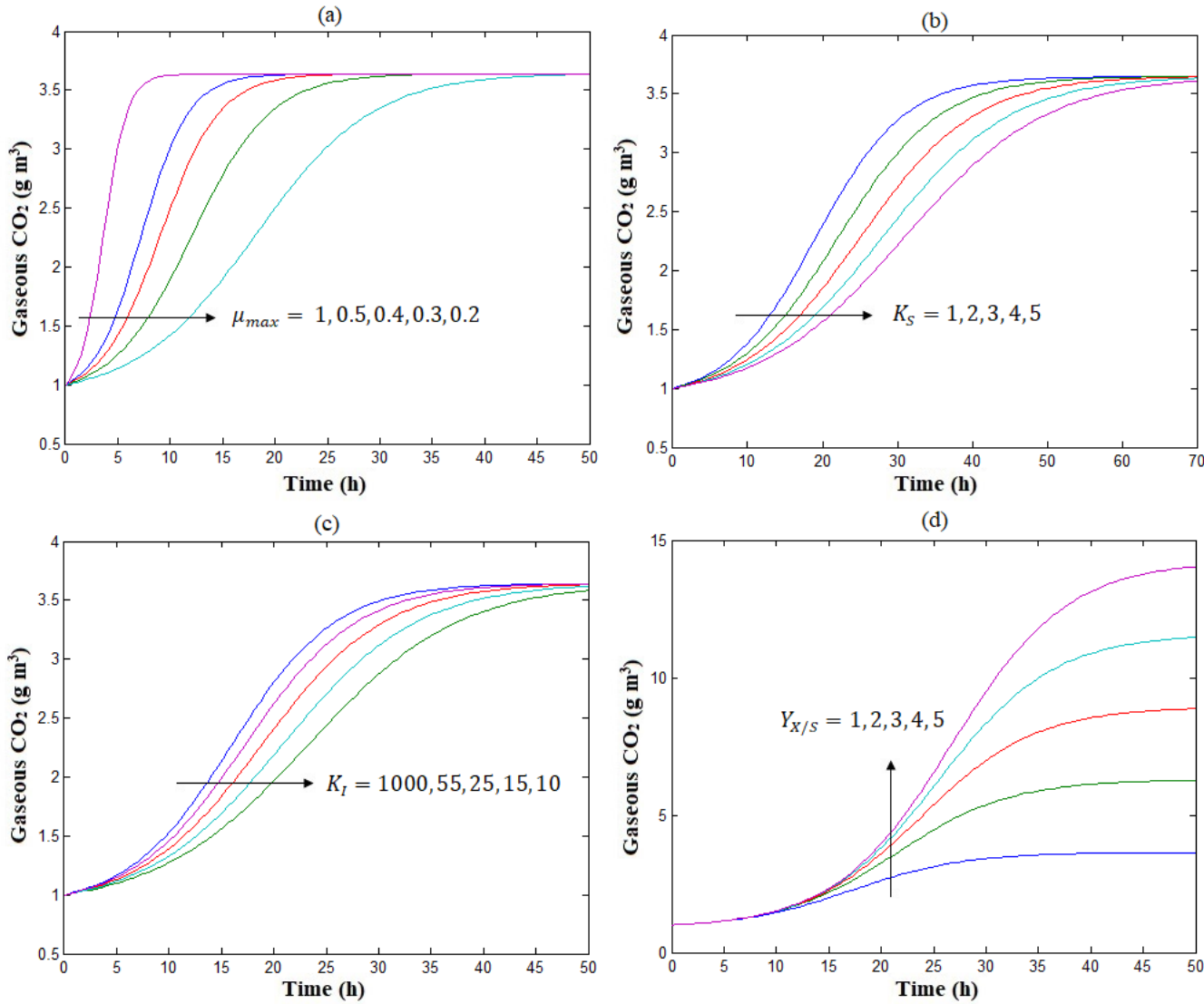


**Fig. 6** Concentration profile of liquid carbondioxide  $CO_{2G}(t)$  [Eq. (12)] versus time  $t$  for some experimental values of the parameters and for various values of (a) maximum specific growth rate  $\mu_{max}$  (b) toluene half saturation constant  $K_S$  (c) toluene inhibition constant  $K_I$  and (d) biomass to toluene yield  $Y_{X/S}$  respectively.